

RSC Advances



This is an *Accepted Manuscript*, which has been through the Royal Society of Chemistry peer review process and has been accepted for publication.

Accepted Manuscripts are published online shortly after acceptance, before technical editing, formatting and proof reading. Using this free service, authors can make their results available to the community, in citable form, before we publish the edited article. This *Accepted Manuscript* will be replaced by the edited, formatted and paginated article as soon as this is available.

You can find more information about *Accepted Manuscripts* in the [Information for Authors](#).

Please note that technical editing may introduce minor changes to the text and/or graphics, which may alter content. The journal's standard [Terms & Conditions](#) and the [Ethical guidelines](#) still apply. In no event shall the Royal Society of Chemistry be held responsible for any errors or omissions in this *Accepted Manuscript* or any consequences arising from the use of any information it contains.

Synthesis of 1D upconversion CeO₂: Er, Yb nanofibers via electrospinning and its performance in dye-sensitized solar cells

Jingyi Bai, Rongfang Zhao, Gui Han, Zhongcui Li and GuowangDiao*

College of Chemistry and Chemical Engineering, Yangzhou University, Yangzhou, Jiangsu 225002, PR China

Abstract

1D Upconversion CeO₂: Er, Yb nanofibers, which could absorb NIR light and upconvert it to visible light, for increasing the photocurrent of DSSCs has been fabricated by electrospinning method. The products were confirmed by transmission electron microscopy (TEM), high-resolution TEM (HRTEM) and X-ray diffraction (XRD), and fluorescence spectroscopy (PL) techniques. An enhancement of light harvesting efficiency was observed to 14% due to the upconversion and scattering effect. It is anticipated that this nanostructures may provide a new direction for CeO₂ application in DSSCs.

Introduction

Dye-sensitized solar cells (DSSCs) have drawn considerable attention for decades because of their high-efficiency and potential for manufacturing at a low cost [1, 2]. Over the past decades, extensive efforts have been focused on the improvement of their photoelectric conversion efficiency by optimizing the structure and properties of the photoelectrode [3, 4]. The photoelectrode is one of the most important components in the DSSC because the amount of light absorbed in the DSSC is dependent on the absorption spectrum of the photoelectrode. Generally, conventional photoelectrode of DSSCs is composed of TiO₂ nanoparticles with a small size of 20–40 nm. However, due to their small size, the scattering effects are negligible for visible light. Hence, large proportion of incident light would not be utilized in solar cells, and resulting in a low light harvesting efficiency [5-8]. To date, an effective way to enhance the light harvesting capability is to introduce a scattering layer on top of the transparent TiO₂ layer. But the most absorption is in the visible region of the total solar irradiation, which means that approximately 50% of solar irradiation energy in the ultraviolet (7%) and infrared region (43%) is not utilized [9-11]. Therefore, the main constraints for true utilization of solar and the improvement of efficiency is the spectral mismatch between the incident solar photon spectrum and the semiconductor's band gap[12]. Considering to resolve this problem is modifying the solar energy spectrum via luminescence phenomenon to the wavelength range, and in this range the solar cells can get high absorption probability. The solar spectrum adjustable results in efficiency enhancement of solar cell through downconversion and especially upconversion [13-16]. Upconversion phenomenon refers to nonlinear optical processes in which the sequential adsorption of two or more photons leads to the mission of light at shorter wavelength than the excitation wave length (anti-Stokes emission) [17, 18]. It is well known that the NIR irradiation and nonradiative relaxation of excited ion can generate thermal energy. Meanwhile, solar cells generally operate at high temperature. It is reasonable to expect that the more thermally stable, green metal oxide will play an important role [19]. A great deal of research effort has been focused on the upconversion materials NaYF₄: Ln

*Corresponding author. E-mail: gw_diao@yzu.edu.cn.

(Ln=Yb, Er and Tm) because of their low phonon energy, which suppresses nonradiative transition of excited electrons [20, 21], but the stable and nontoxic oxide upconversion materials are preferable to fluoride. The CeO₂:Ln upconversion nanomaterials using in DSSC remains largely unexplored, and CeO₂ normally is such a cheap materials with nontoxic and high stable property in the family of rare earth oxide, which has been widely used for many regions, it is reasonable that CeO₂ also has been considered as a useful host for phosphors activated with lanthanide ions[22-24]. In addition, CeO₂ has low phonon energy and the ionic radius of Er³⁺ and Yb³⁺ is very close to Ce⁴⁺. It is easy to introduce the Er³⁺ and Yb³⁺ into the Ce⁴⁺ host lattice [25]. In this paper, 1D upconversion CeO₂: Er, Yb nanofibers were prepared by electrospinning and tested for the light scattering materials and further clarify the effect of upconversion materials in our system, so that the efficiency of solar cells can be increased.

Experimental

Synthesis of 1D upconversion CeO₂: Er, Yb nanofibers

To synthesize CeO₂: Er, Yb luminescent nanofibers, all the chemicals reagents used in experiments were of analytical grade and used as received without further purification. In order to obtain uniform 1D morphology, electrospinning method is used. By adjusting some of the electrospinning parameters, 1D hybrid fiber-like precursor materials was fabricated. First, 1.2 g polyvinylpyrrolidone (PVP, 30kDa), and 4ml N,N-dimethyl-formamide (DMF) were dissolved in 10 g ethanol, then 1ml 2.5M Ln(NO₃)₃ (Ln=Ce, Yb and Er) was slowly added to the above solution with stirring at room temperature to form uniform polymer solution. Under applied electrical force, the polymer solution is ejected from the needle, and the solvents are evaporated, the samples are collected on a grounded collector. A high temperature annealing is employed to remove the organic polymer templates to obtain pure 1D inorganic nanofibers. The 1D hybrid fiber-like precursor materials PVP/CeO₂: Er, Yb was annealed at 1150°C for 3h to remove the organic polymer templates, and the resulting powders were 1D upconversion luminescence CeO₂: Er, Yb nanofibers. For comparison, the CeO₂ undoped with Er, Yb nanofibers was obtained by the same route without the addition of Er(NO₃)₃ and Yb(NO₃)₃ solution.

Characterization

High-resolution TEM (HRTEM) and Energy dispersive X-ray (EDX) were performed on a FEI Tecnai G2 F30 STWIN (U.S.A.) operating at 200 kV. Diffraction (XRD) data were obtained with a graphite monochromator and Cu K α radiation ($\lambda = 0.1541$ nm) on a D8 advance superspeed powder diffractometer (Bruker). X-ray photoelectron spectra (XPS) were recorded by ESCALAB250Xi spectrometer (ThermoFisher, America). The upconversion photoluminescence spectra were measured by the shimadzu 4500 fluorescence spectrophotometer combined steady state fluorescence, using a 980nm laser as the excitation source. The morphologies and microstructures of the samples were investigated by field-emission scanning electron microscope (FESEM) using a Hitachi S-4800 (Japan) apparatus and transition electron microscopy (TEM) on a Philips TECNAI-12 instrument under an acceleration voltage of 200 kV. Solar energy conversion efficiency was measured using solar simulator (Oriel Sol 3A Solar Simulator, 94063A, Newport Stratford Inc. USA).

Fabrication of photoelectrode and the assembly of DSSCs

The photoelectrode films of commercial P25 (Degussa) were prepared by adding P25, triton X-100 and 2,4-Pentanedione to the terpineol solution of ethyl cellulose, and coated on a conducting glass with F:SnO₂ film (FTO, 7 Ω /aq) using a doctor-blade printing technique. The pre-treatment

with TiCl_4 was applied to the FTO glass, through immersing in TiCl_4 solution at 70°C for 30min, and then printing TiO_2 paste. After printing, the electrode was dried at 60°C . In order to obtain the paste for the scattering layer, the CeO_2 : Er, Yb upconversion nanofibers were added into the solution containing terpineol, ethyl cellulose and stirred for 1 h, which were pasted onto the TiO_2 transparent layer. Finally, the modified photoelectrode were sintered in a muffle at 450°C . After cooling to 80°C , the electrode was immersed into dye solution (N719, dyesol, Australia 0.5mM in acetonitrile) and kept at the room temperature for 24hr. Then, the dye-adsorbed electrode was washed with ethanol and dried. Platinum counter electrode was prepared by conventional thermal decomposition method using H_2PtCl_6 precursor onto FTO glass. The liquid electrolyte was composed of LiI (0.1 M), I_2 (0.05 M) and TBP (0.5 M) in acetonitrile.

Results and discussion

Fig.1a shows the XRD patterns of CeO_2 : Er, Yb nanofibers, and All the reflection peaks could be readily indexed to pure cubic fluorite CeO_2 (JCPDS Card No. 34-0394). No diffraction peaks for Er_2O_3 or Yb_2O_3 was observed in the materials, which might confirms the formation of a single phase resulting in successful doping of Er, Yb ions into ceria. As shown in PXRD pattern of the strongest diffraction peaks of the CeO_2 : Er, Yb in Fig.1b, the intensity and the position of peaks are different each other, such peak shifts reflect little changes in the crystal lattices of host materials and can be caused by incorporating alien ions with sizes different to those of the host ions. The peak become sharper with increasing concentrations of Er when the value of Yb is consistent. When the content value is Ce: Er: Yb=96.7:3:0.3, the highest intensity of diffraction peak are obtained.

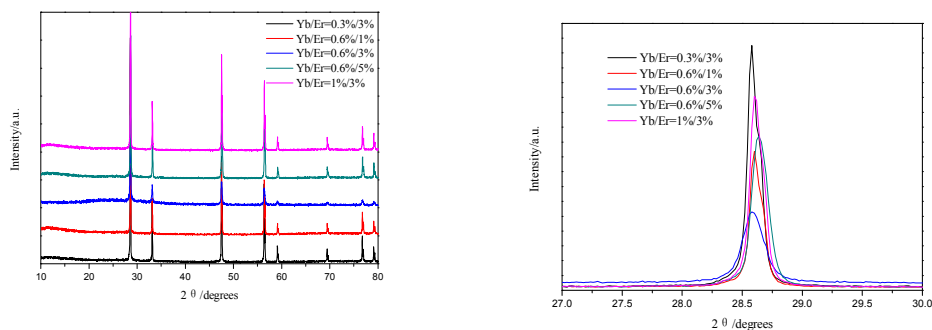


Fig.1 (a) XRD patterns of the CeO_2 : Er, Yb nanofibers with different ratios of Yb/Er, (b) PXRD patterns of the strongest diffraction peaks of the CeO_2 : Er, Yb nanofibers with different ratios of Yb/Er

To elucidate the elemental composition of the CeO_2 : Er, Yb nanofibers XPS analysis was used. The peak position of different atoms are shown in Fig.2. Fig. 2a shows the wide scan of this materials, the binding energy for Ce (3d) and Er (4d) can be noted. As shown in Fig.2b and 2c, several Ce 3d peaks corresponding to Ce^{3+} (901.4 and 883.1eV), Ce^{4+} (917.1 and 898.9eV) and Er^{3+} (168.2eV) mean the existence of Ce^{3+} and Er^{3+} in the lattice of CeO_2 : Er, Yb nanofibers. The Yb peak is not detected because of the small concentration of Yb in the nanofibers.

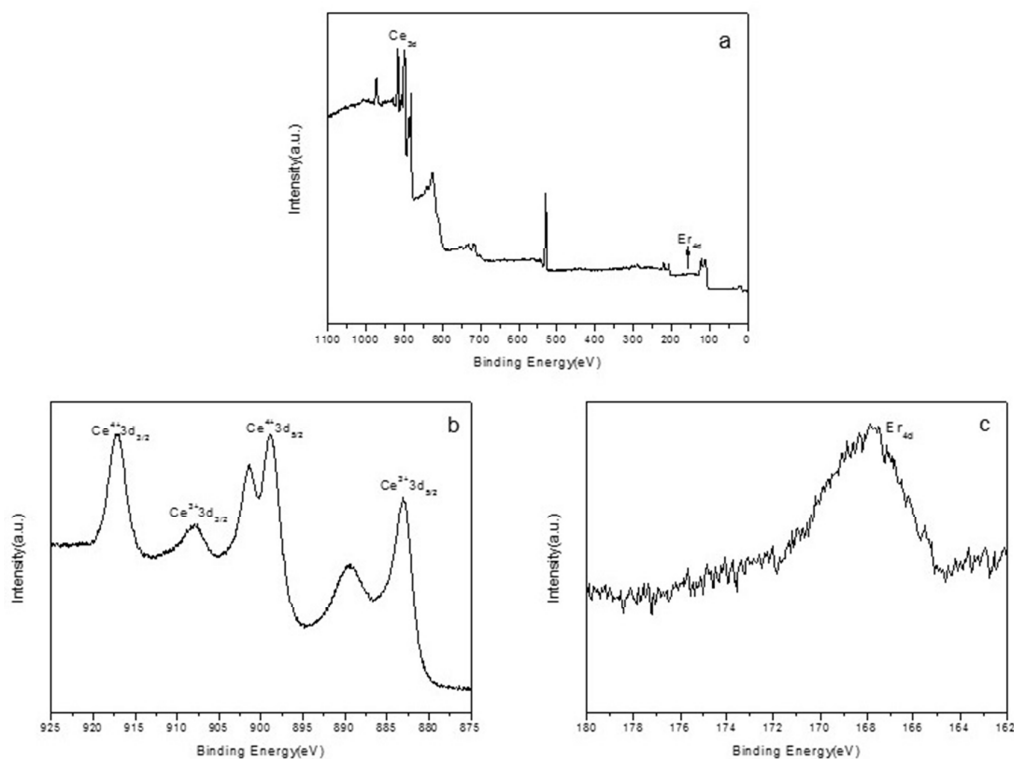


Fig.2 XPS spectrum of CeO₂: Er, Yb nanofibers(a), Ce 3d region (b) and Er 4d region (c)

The EDS analysis was employed to investigate the chemical composition and purity of as-synthesized CeO₂: Er, Yb nanofibers. The pattern of Ce_{0.967}O₂: Er_{0.03}, Yb_{0.003} nanofibers shown in Fig.3, reveals that there only exist elements Ce, O, Yb and Er, no other element were detected in the spectrum.

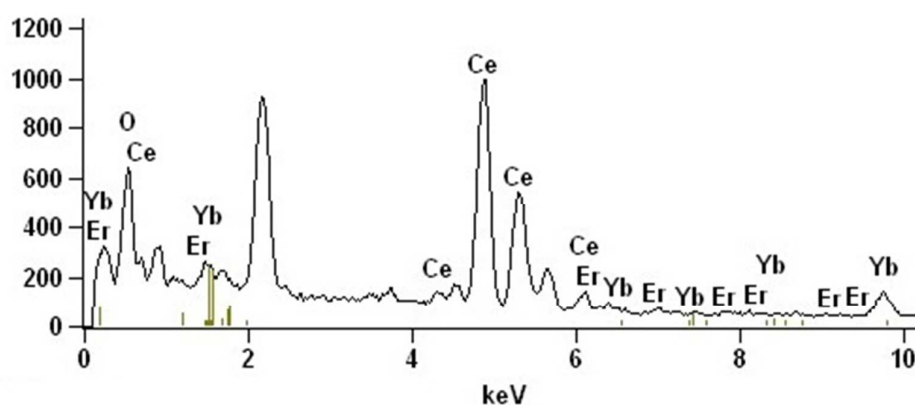


Fig.3 EDS spectra of CeO₂: Er, Yb nanofibers

The typical SEM, TEM and HRTEM images of CeO₂: Er, Yb nanofibers are shown in Fig.4. From the SEM micrograph, it can be seen that the as-formed precursor fibers are uniform with diameters ranging from 300-400nm. After being calcined at 1150°C for 3h, the fibers shrink and become

curvy due to the decomposition of PVP and crystallization of ceria oxide. It can be found from Fig.4(c), (d) that 1D nanofibers consist of particles with size of about 80-100 nm. The corresponding HRTEM image in Fig.3e revealed that the particles in upconversion nanofibers have well lattice planes and good crystallinity. The d-spacing of 0.34nm was well consistent with those of pure cubic CeO_2 phase. These results further confirm the formation of the 1D upconversion CeO_2 : Er, Yb nanofibers.

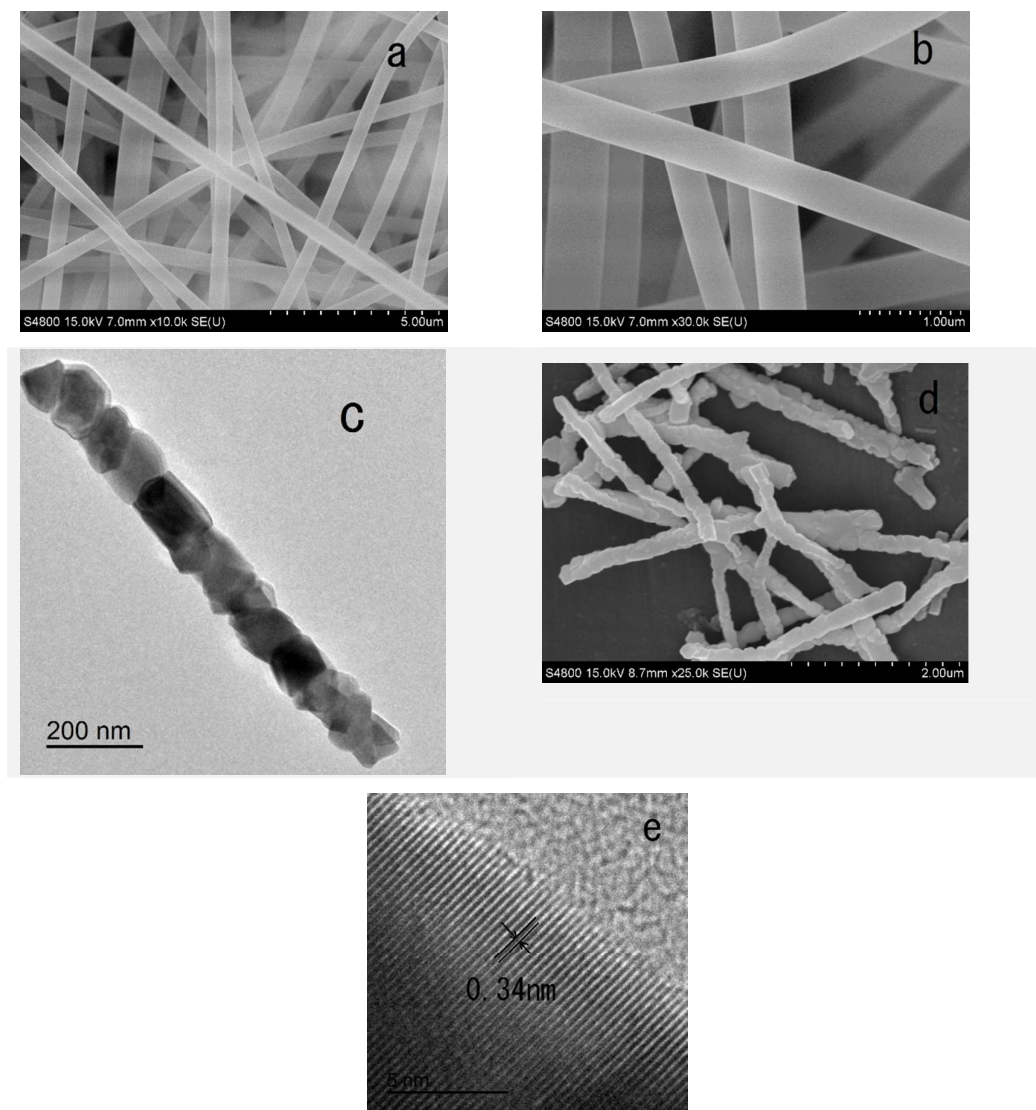


Fig.4 SEM images of (a),(b) 1D hybrid fiber-like precursor materials PVP/ CeO_2 : Er, Yb, (c),(d) TEM and SEM images (e) HRTEM image of CeO_2 : Er, Yb nanofibers after calcination at 1150°C

The room temperature PL spectra of 1D CeO_2 : Er, Yb nanofibers with different ratio of Yb/Er recorded in alcohol and following excitation at 980nm is shown in Fig.5. The most intense spectral green peaks located at 525nm, 550nm and 562nm, which was attributed to the energy transitions from $^2\text{H}_{11/2}$ and $^4\text{S}_{3/2}$ to $^4\text{I}_{15/2}$. The red peak at 660nm and 680nm correspond to the

energy transitions from $^4F_{9/2}$ to $^4I_{15/2}$ of Er^{3+} ions, respectively, which were excited by using a commercial continuous wave diode 980nm laser. According to the emission spectra, the relative photoluminescence intensity of 1D CeO_2 : Er, Yb nanofibers is enhanced with better crystallinity along with enhanced v-v separation after raising the activator in host lattice. But larger concentrations of Er^{3+} do not increase the PL intensity because of filling the quenching sites.

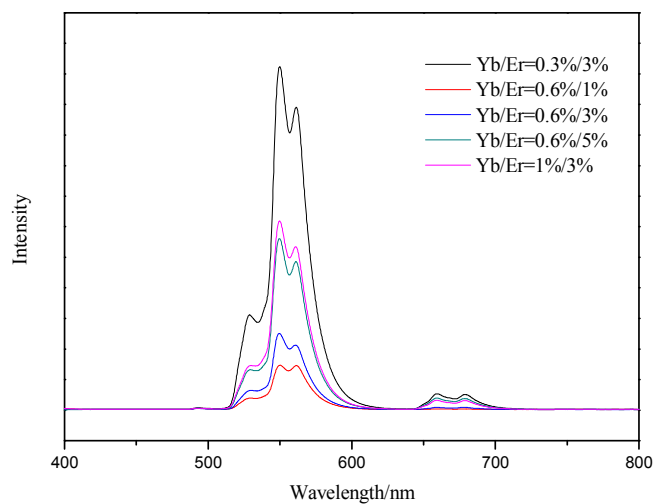


Fig.5 The upconversion emission spectrum of the CeO_2 : Er, Yb nanofibers with different ratios of Yb/Er

In order to investigate the DSSC performance of the sample, bilayer films were constructed by printing an upconversion layer and CeO_2 undoped with Er, Yb nanofibers layer on the top of layer P25. The photocurrent density–voltage curves (J–V) of DSSCs based on different photoelectrodes are shown in Fig.6, and their photovoltaic parameters are summarized in Table 1. Under illuminating to $100\text{mW}/\text{cm}^2$ solar spectrum, the uncoated solar cell had a short current density (J_{sc}) of $11.43\text{mA}\cdot\text{cm}^{-2}$, open circuit voltage (V_{oc}) of 0.730V and a Fill Factor (FF) of 0.693 with an efficiency (η) of 5.791%, while for the solar cells with an unconversion layer, J_{sc} of $12.65\text{mA}\cdot\text{cm}^{-2}$, V_{oc} of 0.723V, FF of 0.729 and η of 6.661% were obtained. Therefore, the solar cell coated with luminescent film, improved the current density and energy conversion efficiency with an increase of 10.6% and 15.02%, respectively. The DSSCs composed of CeO_2 undoped with Er, Yb nanofibers layer had a J_{sc} of $12.046\text{mA}\cdot\text{cm}^{-2}$, V_{oc} of 0.724V, FF of 0.706 and η of 6.158% respectively.

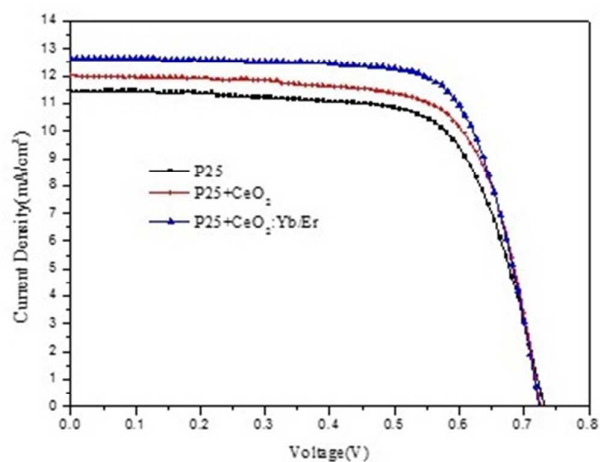


Fig. 6. The photocurrent-voltage curves of dye-sensitized solar cells without upconversion layer, with CeO_2 undoped with Er,Yb nanofibers layer and with upconversion layer.

	$J_{sc}(\text{mA}/\text{cm}^2)$	$V_{oc}(\text{V})$	FF	$\eta\%$
P25	11.436	0.730	0.693	5.791
P25+ CeO_2	12.046	0.724	0.706	6.158
P25+ CeO_2 :Yb/Er	12.647	0.723	0.729	6.661

Table 1 Detailed photovoltaic characteristics of DSSCs based on different photoelectrodes

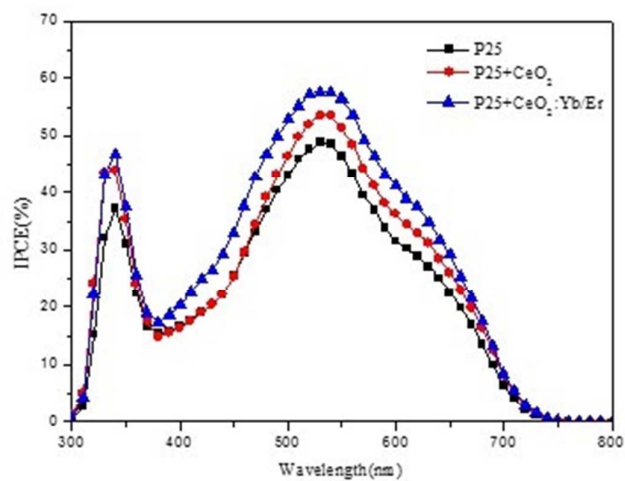


Fig.7. IPCE spectra of DSSCs without upconversion layer, with CeO_2 undoped with

Er,Yb nanofibers layer and with upconversion layer.

Fig.7 shows the typical curves of IPCE in the 300-800nm wavelength range. It indicates that when the upconversion layer is coated onto P25 film the IPCE increases, which is caused by the upconversion and scattering effect. By adding the CeO₂ undoped with Er, Yb nanofibers layer, the IPCE also increases compared with P25 film, which can be totally attributed to the light scattering effect. The phenomenon of light scattering effect can also be drawn by the color of the photoelectrode which were immersed into N719 dye solution. The electrode without upconversion layer has the same color at both sides owing to the bare P25 nanoparticles, which means that the dye absorbed evenly. Whereas, the color of the side with upconversion layer is different with another side because of the big size of upconversion CeO₂: Er, Yb nanoparticles, and the dye absorbed onto the big size particles is not enough than the small size P25 particles. However, the IPCE of DSSCs by adding the CeO₂ undoped with Er, Yb nanofibers layer still lower than those composed of upconversion CeO₂: Er, Yb nanofibers layer, therefore, the enhancement of current and efficiency may be due to light absorption of the upconversion induced DSSCs.

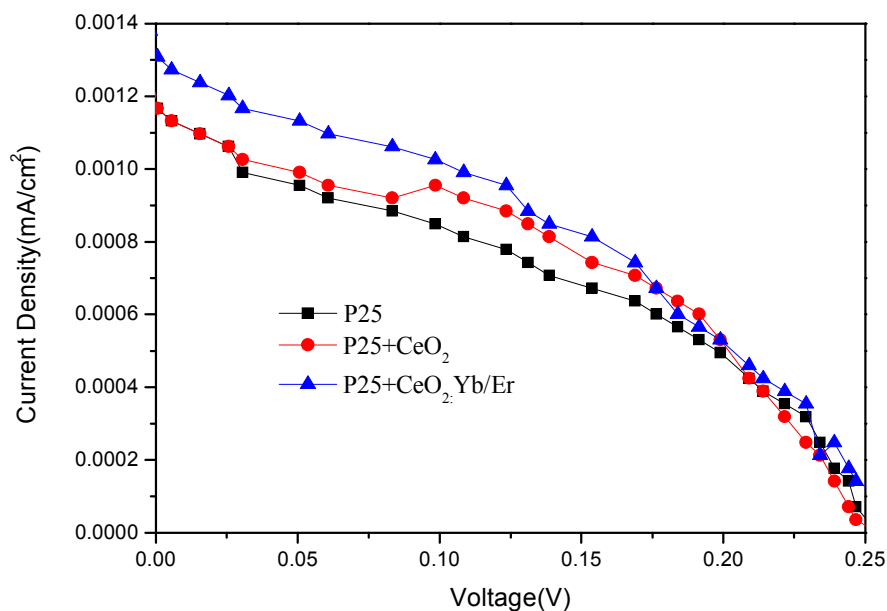


Fig.8 I-V curve of DSSCs under illumination with a 2W power 980nm laser

This remarkable reflectance is obviously attributed to the strong mirror-like scattering with the large cubic CeO₂ facets, on which the incident light can directly be reflected backwards. To confirm the fact that the upconversion layer composed DSSCs can utilize the NIR light and generate photocurrents, the I-V curve of the DSSCs with upconversion layer and without layer P25 photoelectrode under 980nm light are also measured, little photocurrent is produced in the photoelectrode composed DSSCs in P25 layer about 0.001mA·cm⁻², but the photocurrent with upconversion layer is about 0.0013mA·cm⁻², the increased J_{sc} should be attributed to the upconversion effect.

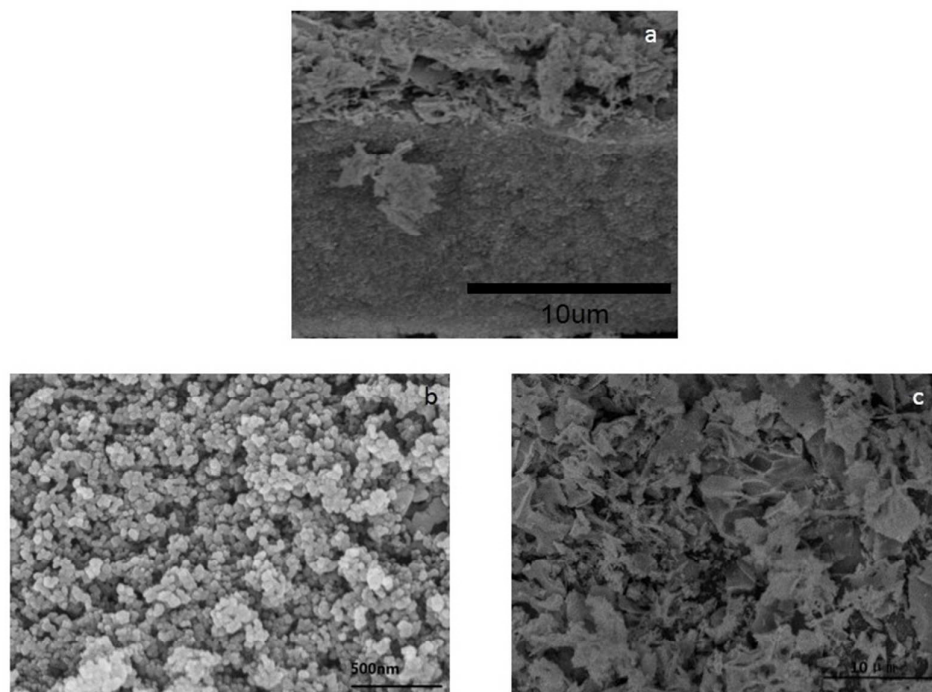


Fig.9 SEM images of cross-section of the bilayer photoelectrode (a), TiO₂ layer (b) and CeO₂:Er, Yb nanofibers layer (c)

Fig.9 shows the SEM images of the bilayer photoelectrode. An overview of the bilayer photoelectrode (Fig.9a) indicates that the bifunctional scattering and upconverting layer is coated on the surface of the dense TiO₂ film. From Fig.9b, mesoporous particles of TiO₂ were uniformly and densely distributed on the surface. As can be observed in Fig.9c, during the fabrication of the upconversion layer, the CeO₂:Er, Yb upconversion nanofibers were oriented and fused with each other, large assemblies were formed. Another reason for the assemblies is deduced because of triton X-100 and terpineol solution of ethyl cellulose when DSSCs were fabricated.

Conclusion

In conclusion, 1D CeO₂:Er, Yb upconversion nanofibers were designed and fabricated by electrospinning for making more efficient DSSCs. Compared to the P25 photoelectrode, the efficiency of DSSCs with CeO₂:Er, Yb layer is as large as 15% enhancement. It can be observed that the utilization of the CeO₂:Er, Yb nanofibers leads to an increase in the overall photocurrent of the solar cells under simulated sunlight irradiation. Apart from using as an upconversion materials to harvest the NIR light, it can also serve as a scattering materials to enhance the absorbance of the solar cells.

Acknowledgement

This work was financially supported by the National Natural Science Foundation of China (Grant 20973151, 20901065, and 21273195), a Project Funded by the Priority Academic Program Development of Jiangsu Higher Education Institutions. The authors also acknowledge the Testing Center of Yangzhou University for SEM and EDS experiments.

References

- 1 M. Grätzel, *Nature*, 2001, **414**, 338.

- 2 B. O'Regan and M. Grätzel, *Nature*, 1991, **353**, 24.
- 3 B.M.van der Ende, L.Aarts, A.Meijerink, *J. Phys. Chem. Phys.*, 2009, **11**, 11081
- 4 C.Strumpel, M.Mccann, G.Beaucarne, VArkipov, A. Slaoui, V.Svrcek, C.Delcanizo, I. Tobias, *Sol. Energy Mater. Sol. Cells*, 2007, **91**, 238.
- 5 Y. C. Park, Y. J. Chang, B. G. Kum, E. H. Kong, J. Y. Son, Y. S. Kwon, T. Park and H. M. Jang, *J. Mater. Chem.*, 2011, **21**, 9582.
- 6 H. Yu, Y. Bai, X. Zong, F. Q. Tang, G. Q. M. Lu and L. Z. Wang, *Chem. Commun.*, 2012, **48**, 7386.
- 7 Z.Y. Zhou, J.H. Wang, F. Nan, C. H. Bu, Z. H. Yu, W. Liu, S. S. Guo, H. Hu and X. Z. Zhao, *Nanoscale*, 2014, **6**, 2052.
- 8 C. Z. Yuan, G. Y. Chen, Paras N. Prasad, Tymish Y. Ohulchansky, Z.J. Ning, H. N.Tian,LichengSund and Hans Agren, *J. Mater. Chem.*, 2012, **22**, 16709.
- 9 R. Levinson, P. Berdahl, H. Akbari, *Sol. Energ. Mater. Sol. C*, 2005, **89**, 351.
- 10 R. Levinson, P. Berdahl, H. Akbari, *Sol. Energ. Mater. Sol. C*, 2005, **89**, 319.
- 11 W. Qin, D. Zhang, D. Zhao, L. Wang and K. Zheng, *Chem. Commun.*, 2010, **46**, 2304.
- 12 M.Zahedifar, Z. Chamanzadeh, S. M. Hosseinpoormshkani, *Journal of luminescence*, 2013, **135**, 66.
- 13 E. Klampaftis, D. Ross, K.R. Macintosh, B.S. Richards, *Sol. Energy Mater. Sol. Cells*, 2009, **93**, 1182.
- 14 P. Ramasamy, P. Manivasakan, J.W. Kim, *RSC Advances*, 2014, **4**, 34873
- 15 M. Liu, Y. Lu, Z.B. Xie, G.M. Chow, *Sol. Energy Mater. Sol. Cells*, 2011, **95**, 800.
- 16 D. Li, C. Ding, H. Shen, Y. Liu, Y. Zhang, M. Li, *J. Phys. D: Appl. Phys.*, 2010, **13**, 015101.
- 17 F. Wang, X. Liu, *J. Am. Chem. Soc.*, 2008, **130**, 5642.
- 18 J.W. Stouwdam, F. van Veggel, *Nano Lett.*, 2002, **2**, 733.
- 19 X. M. Li, F. Zhang, D.Y. Zhao, *Nano Today*, 2013, **8**, 643.
- 20 K. W. Kramer, D. Biner, G. Frei, H. U. Gudel, M. P. Hehlenand S. R. Luthi, *Chem. Mater.*, 2004,**16**,1244.
- 21 J. F. Suyver, J. Grimm, M. K. van Veen, D. Biner, K. W.Kramer and H. U. Gudel, *J. Lumin.*, 2006,**117**, 112.
- 22 S. Song, L. Xu, Z.Q. He, J.M. Chen, *Environ. Sci. Technol.*, 2007, **41**, 5849.
- 23 F.B. Li, X.Z. Li, M.F. Huo, K.W. Cheah, W.C.H. Choy, *Appl. Catal. A*, 2005, **285**,181.
- 24 A.K. Sinha, K. Suzuki, *J. Phys. Chem. B*, 2005, **109**, 1708.
- 25 H.J. Wu, Z. W. Yang , J.Y. Liao, S.F.Lai, J. B. Qiu, Z. G. Song, Y. Yang, D. C. Zhou, Z. Y. Yin, *J. Alloy. Compd.*, 2014, **586**, 485.